

Multiple-Stripe Lithiation Mechanism of Individual SnO₂ Nanowires in a Flooding Geometry

Li Zhong,² Xiao Hua Liu,¹ Guo Feng Wang,² Scott X. Mao,² and Jian Yu Huang^{1,*}

¹Center for Integrated Nanotechnologies, Sandia National Laboratories, Albuquerque, New Mexico 87185, USA

²Department of Mechanical Engineering and Materials Science, University of Pittsburgh, Pittsburgh, Pennsylvania 15261, USA

(Received 28 February 2011; published 15 June 2011)

The atomic scale lithiation mechanism of individual SnO₂ nanowires in a flooding geometry was revealed by *in situ* transmission electron microscopy. The lithiation was initiated by the formation of multiple stripes with a width of a few nanometers parallel to the (020) plane traversing the entire wires, serving as multiple reaction fronts for later stages of lithiation. Inside the stripes, we identified a high density of dislocations and enlarged interplanar spacing, which provided an effective path for lithium ion transport. The density of the stripes increased with further lithiation, and eventually they merged with one another, causing a large elongation, volume expansion, and the crystalline-to-amorphous phase transformation. This lithiation mechanism characterized by multiple stripes and multiple reaction fronts was unexpected and differed completely from the expected core-shell lithiation mechanism.

DOI: 10.1103/PhysRevLett.106.248302

PACS numbers: 82.47.Aa, 66.30.H-

Understanding the atomic scale lithiation process is the key to unfolding the operation mechanism of lithium ion batteries (LIBs), thus providing the critical science for designing better LIBs [1,2]. Although lithiation has been investigated extensively by theoretical simulation over a wide range of electrode materials [3–14], there is a lack of direct experimental evidence and fundamental understanding of the initiation and evolution of the atomic scale lithiation mechanisms [15,16]. We have demonstrated very recently that it is possible to study the lithiation process at an atomic scale and in real time by TEM [17]. Direct visualization of the lithiation process can provide important insight into how LIBs work and guide the development of advanced LIBs for powering future electrical vehicles and electrical devices.

In a recent publication, we created a nanoscale battery (Fig. S1 in [18]) consisting of a single nanowire anode, an ionic liquid based electrolyte (ILE), and a LiCoO₂ cathode, and conducted *in situ* charging or discharging experiments on an individual SnO₂ nanowire anode inside a TEM. However, in that experiment, one end of the nanowire is in contact with the electrolyte as illustrated in Fig. S2(a) in [18] (hereafter referred to as an “end contact”). Therefore, the lithiation is featured by a single reaction front advancing in the axial direction [Fig. S2(b) in [18]]. However, in a real battery, the nanowires were immersed entirely in the electrolyte in a flooding geometry [hereafter interchangeably referred to as “flooding” or “side contact”; Fig. S2(c) in [18]]. One fundamental question that needs to be addressed is, does the same lithiation mechanism operating in the end contact also operate in a flooding geometry? It is speculated that the previously observed large elongation during charging of SnO₂ nanowires might be related to the end-contact geometry, as it is expected that in an end-contact geometry the reaction interface is perpendicular to the nanowire axis, and the elongation should occur in a direction that is perpendicular to the reaction interface, thus the observed

superelongation [Fig. S2(b) in [18]]. In a similar vein, when the nanowire is flooded in the electrolyte, it is expected to swell rather than elongate [Fig. S2(d) in [18]] [19,20]. To clarify the above argument, we conducted further experiments under both the end-contact and the side-contact (flooding) geometries.

Figure 1 shows morphology and structure evolution of a SnO₂ nanowire anode during the lithiation process in a partially flooded geometry. The initial single crystalline nanowire was 45 μm long and 220 nm thick [Figs. 1(a) and 1(o)]. About 1/3 of the nanowire was immersed into the ILE, and the rest of the nanowire was out of the ILE [Fig. 1(b)]. A -3.5 V bias was then applied to the anode with respect to the LiCoO₂ cathode, which initiated an electrochemical charge in the nanowire. The reaction front (marked by red arrowheads) moved along the nanowire from the ILE side (right) to the substrate (left) [Figs. 1(c)–1(k)]. As the reaction front passed by, the nanowire became bent and twisted. Surprisingly, the flooded segment showed similar morphology to the nonflooded segment with elongation, spiral, buckling, and twist after the ILE was retracted [Fig. 1(l)]. Electron diffraction patterns (EDPs) corresponding to the nonflooded [Fig. 1(m)] and flooded [Fig. 1(n)] segments indicated both reaction products composed of small Sn and Li_xSn particles dispersed in an amorphous Li₂O matrix. Similar results were obtained in many other flooding tests (e.g., Fig. S3 in [18]). Again, we saw similar morphology changes in the flooded and nonflooded segments after lithiation, both undergoing similar elongation and swelling, and exhibiting a typical amorphous gray contrast [Figs. S3(l) and S3(m) in [18]]. Elongation of the flooded segment was also measured in Fig. S3 in [18]. With two reference marks visible before and after charging in the flooded segment [Figs. S3(j) and S3(k) in [18]], the elongation of the flooded segment after charging was estimated to be 65%, comparing to a 60% total elongation of the whole

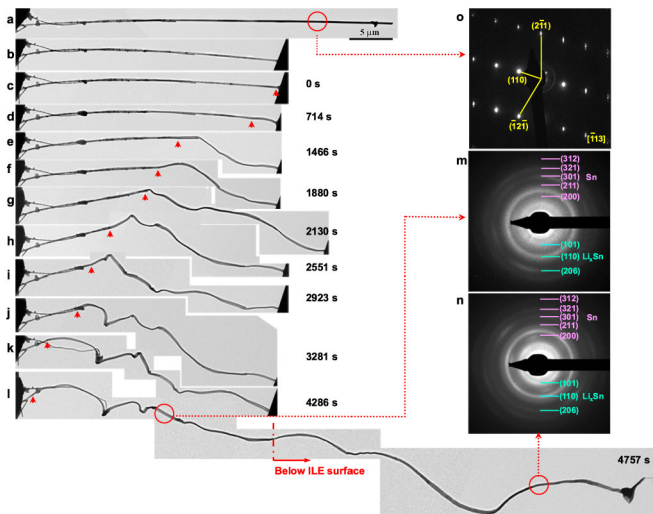


FIG. 1 (color online). Structure evolution of a SnO_2 nanowire anode in a flooding geometry during charging at -3.5 V with respect to the LiCoO_2 cathode. (a) A $45 \mu\text{m}$ long and 220 nm thick pristine SnO_2 nanowire with single crystalline structure (o). (b) Flooding geometry in which about $1/3$ of the nanowire was immersed in the ILE. (c)–(k) Sequential images showing the morphology change during charging. The reaction front (indicated by the red arrowheads) progressed continuously along the nanowire's axial direction. (l) Lithiated nanowire after the ILE was withdrawn. Similar morphology was observed for both the flooded and the nonflooded segments. The corresponding EDPs of nonflooded (m) and flooded (n) segments showed almost identical structure after lithiation.

nanowire, indicating a 55% elongation of the nonflooded segment, which is consistent with that measured from the *in situ* experiments [17].

To understand further the lithiation mechanism in a flooding geometry, we stopped lithiation at various intermediate stages and retracted ILE to inspect the structure evolution of the flooded segment. Figure 2 shows morphology and structure changes at different lithiation stages of several SnO_2 nanowires in a flooding geometry. A pristine SnO_2 nanowire was smooth and straight, with a single crystalline rutile structure before lithiation [Figs. 2(a) and 2(g)]. After a -3.5 V bias was applied to the SnO_2 nanowires against a LiCoO_2 cathode, there were no detectable changes until after approximately 90 s, when a set of dark-contrasted stripes inclined 61° with respect to the side surface of the nanowire emerged [Fig. 2(b)]. After a few more seconds, the spacing between the stripes became smaller and there was dislocation contrast all over the nanowire [Fig. 2(c)]. These stripes were induced by lithiation. The EDP of the striped nanowire [Fig. 2(h)] showed single-crystal diffraction spots superimposed on a diffuse scattering background caused by inelastic scattering originating from lithiation induced defects. These strips were likely nucleated from local surface regions with atomic scale defects [Fig. S4 in [18]] and each traversed the entire nanowire [Fig. S5 in [18]]. Upon further lithiation, the contrast of these stripes became blurred [red rectangle in

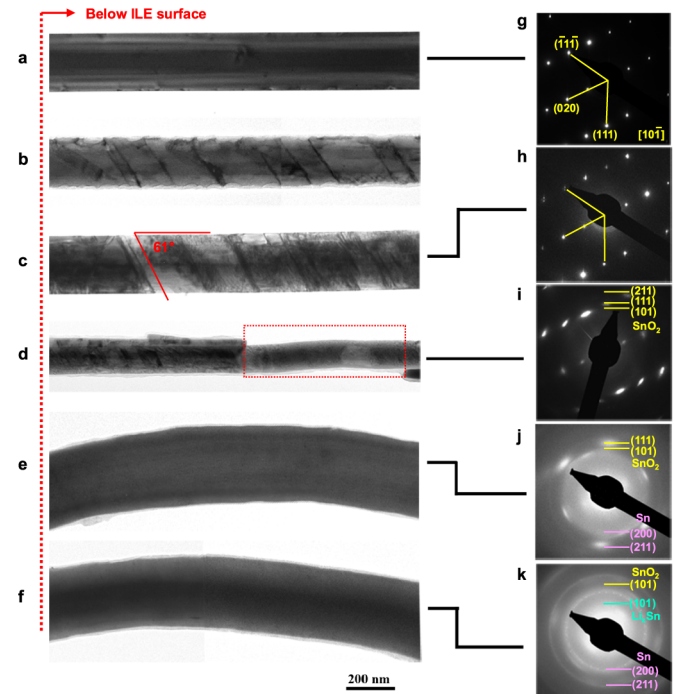


FIG. 2 (color online). Multiple stripe formation in flooded SnO_2 nanowire anodes during charging at -3.5 V against the LiCoO_2 cathode. (a) Pristine single crystalline nanowire and its corresponding EDP (g) which can be indexed to the $[10\bar{1}]$ zone axis of the rutile SnO_2 . (b),(c) Multiple stripes formed after lithiation. A set of parallel stripes with dark contrast inclined 61° to the side surface of the nanowire. The corresponding EDP (h) showed single-crystal diffraction spots superimposed on a diffuse scattering background. Morphology [(d)–(f)] and the corresponding EDPs [(i)–(k)] after further lithiation. After further lithiation, the stripes disappeared completely and the nanowire underwent both elongation and swelling. The corresponding EDP [(j),(k)] showed that the SnO_2 nanowire has been reduced to $\text{Sn} + \text{Li}_2\text{O} + \text{Li}_x\text{Sn}$. Note the images shown in (d)–(f) are from different nanowires immersed in the ILE for different time and all the viewing direction is $[10\bar{1}]$.

Fig. 2(d)]. In the meantime, some weak arcs around the single-crystal diffraction spots emerged [Fig. 2(i)] due to lithiation induced polycrystallization of the nanowire. With further lithiation [Figs. 2(e) and 2(f)], the arcs around SnO_2 diffraction spots became much weaker [Fig. 2(j)] and finally barely discernible [Fig. 2(k)], and the whole nanowire was converted to a Sn , Li_xSn , and Li_2O amorphous matrix [Fig. 2(k)].

It took about 2 – 5 min to fully lithiate a nanowire of $15 \mu\text{m}$ long in a flooding geometry. In comparison, full lithiation of the same length of a nanowire in an end-contact configuration took ~ 30 min. Obviously, the multiple stripes acted as multiple reaction fronts in the side-contact geometry, in contrast to the single reaction front in the end-contact geometry.

It is interesting to note that during the whole lithiation process in a flooding geometry, even though lithium ions diffuse from the surface towards the interior of the

nanowire, the assumed core-shell structure [Fig. S2(d) in [18]] was never observed. Instead, the unexpected multiple stripes and multiple reaction fronts appeared throughout the nanowire, leading to large elongation. Therefore, it is important to understand the nature of the multiple stripes.

Figure 3(a) shows the morphology of a SnO_2 nanowire with [011] growth direction [Fig. S6 in [18]] at the initiation stage of lithiation, again showing multiple stripes inclined to the nanowire axis, and Fig. 3(b) is a high-resolution transmission electron microscopy (HRTEM) image and an EDP of the same nanowire before lithiation. The stripes were parallel to the (020) plane, which was apparently the preferred lithium insertion plane. HRTEM images [Figs. 3(c) and 3(d)] of the same nanowire showed lithiation induced dislocations along the stripe. A possible Burgers vector of the dislocations was determined to be [001] or [100] [21,22]. The lithiation induced dislocation cores may act as fast lithium diffusion channels and may increase the lithiation kinetics [23]. Based on previous studies [4–6,24], [001] is the diffusion channel in a rutile structural crystal such as SnO_2 . Therefore, the initial lithiation process can be interpreted as follows: lithiation initiated at some surface defects, continued along [001] direction in the (020) plane. The lithiation induced stress led to formation of dislocations along the stripes, which further facilitated lithium diffusion into the interior of the nanowire. The multiple-stripe formation process was rather quick and the density of stripes increased with progression of lithiation [Figs. 3(e) and 3(f)]. HRTEM images [Figs. 3(g) and 3(h)] from another striped nanowire identified a high density of dislocations with Burgers vectors of [100] and [001]. The crystal lattice became indiscernible at some areas inside the stripes, indicating the beginning of the reaction to form Sn and amorphous Li_2O . Therefore, lithiation-driven dislocation plasticity in the stripes occurred and was a precursor of the crystalline-to-amorphous phase transition. The dislocation density was estimated to be $\sim 5 \times 10^{16}/\text{m}^2$ based on Fig. 3(h), similar to that in the Medusa zone observed in a nonflooded nanowire [17]. Such a high dislocation density can provide the necessary energy and kinetic pathway towards complete amorphization.

Figure 4 shows the evolution of the lattice spacing changes with lithiation obtained from EDPs. When the stripes formed, the (020) diffraction spots were split in two [Figs. 4(c) and 4(d), and the corresponding insets]. The brighter spot corresponded to a d spacing of 2.36 Å, which matched well with the SnO_2 (020) plane, while the darker spot had a d spacing of 2.43 Å, which was caused by lithiation induced lattice expansion [Fig. 4(c) inset]. With further lithiation, the spot from the pristine lattice became much weaker, and the brighter spot corresponded to a d spacing of 2.49 Å, a $\sim 5.5\%$ increase with respect to the pristine structure [Fig. 4(d) inset]. It confirmed that the transverse (020) plane was the preferred lithiation plane, which may be ascribed to the side-contact geometry as shown in Fig. 4(e). Since the (020) plane traverses the nanowire, lithium ions diffuse into the [001] channels in

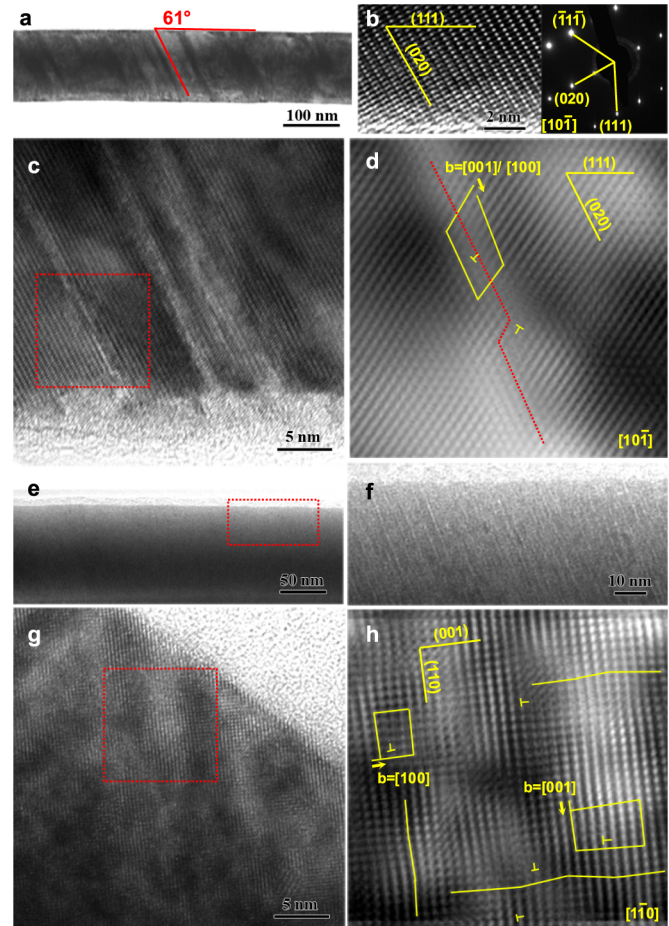


FIG. 3 (color online). Microstructure of the lithiation induced multiple stripes in SnO_2 nanowires. (a),(b) Low and high magnification images of the charged (a) and pristine (b) nanowire. The orientation of the nanowire is $[10\bar{1}]$ zone axis. Stripes inclining 61° to the (111) planes of the nanowire [see also Figs. 2(b) and 2(c)] are parallel to the (020) plane. (c),(d) A raw and a Fourier filtered HRTEM image of the multiple stripes. (d) High magnification image of the framed area in (c), showing dislocations with Burgers vector [001] or [100] in the stripes. (e),(f) Images of the nanowire after further lithiation. (f) High magnification image of the framed area in (e), showing a high density of stripes formed after prolonged lithiation. (g),(h) A raw and a Fourier filtered HRTEM image of another nanowire after lithiation, showing a high density of dislocations with Burgers vectors of [100] and [001], and even disordering. The nanowire is orientated at $[1\bar{1}0]$ zone axis and the growth direction is [011].

the (020) plane inside the nanowire through surface defects. The special one-dimensional geometry of nanowires plays an important role in this multistripe lithiation mechanism. The flexibility in the longitudinal direction and the small diameter facilitate lithium insertion [25–31], leading to easier lithium intercalation along the (020) plane which traverses the nanowire.

In summary, we have conducted *in situ* TEM observation on the lithiation process of SnO_2 nanowires in a flooding geometry. We found a multiple-stripe multiple-reaction-front lithiation mechanism, in which multiple stripes along

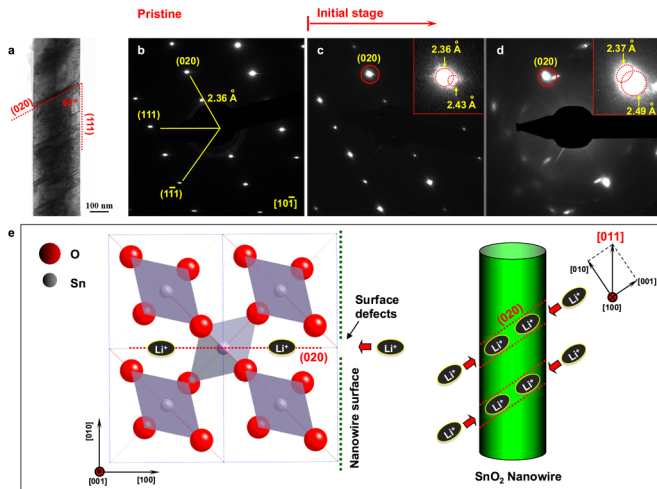


FIG. 4 (color online). EDPs from the striped nanowire indicated lattice expansion caused by lithiation. (a)–(d) Structure evolution viewed from $[10\bar{1}]$ zone axis. (a) Stripes parallel to the (020) plane formed after initial lithiation. (b)–(d) The (020) diffraction spot was split in two with different d spacings [insets in (c) and (d)], with the brighter spot corresponding to a d spacing of 2.36 Å, matching that of the (020) plane in the pristine structure, while the darker spot has a d spacing of 2.49 Å, indicating a 5.5% lattice expansion induced by lithiation. (e) Schematic illustration of lithium intercalation along $[001]$ in the (020) plane in a side-contact geometry. The nanowire's growth direction is $[011]$.

the (020) plane traversing the nanowire were formed. Lattice expansion and dislocations were observed inside the stripes. The nanowires were elongated after lithiation. The new lithiation process that we discovered here has important implications to real lithium ion batteries in which the electrodes are immersed in the electrolyte.

Portions of this work were supported by the Science of Precision Multifunctional Nanostructures for Electrical Energy Storage (NEES), an Energy Frontier Research Center (EFRC) funded by the U.S. Department of Energy (DOE), Office of Science, Office of Basic Energy Sciences under Award No. DESC0001160. The NEES center supported the development of TEM techniques. CINT supported the TEM capability. In addition, this work was performed, in part, at the Sandia-Los Alamos Center for Integrated Nanotechnologies (CINT), a U.S. DOE, Office of Basic Energy Sciences user facility. SNL is a multiprogram laboratory operated by Sandia Corporation, a wholly owned subsidiary of Lockheed Martin Company, for the U.S. DOE's National Nuclear Security Administration under Contract No. DE-AC04-94AL85000. S.X.M. and L.Z. were supported by NSF Grants No. CMMI0825842 and No. CMMI0928517 through the University of Pittsburgh and SNL. We thank Chong Min Wang and Wu Xu from Pacific Northwest National Laboratory for providing the SnO_2 nanowires and the ionic liquid electrolyte.

*Corresponding author.

jhuang@sandia.gov

- [1] S. Choi and A. Manthiram, *J. Electrochem. Soc.* **149**, A1157 (2002).
- [2] M. M. Thackeray *et al.*, *Electrochem. Solid State Lett.* **1**, 7 (1998).
- [3] C. Uthaisar and V. Barone, *Nano Lett.* **10**, 2838 (2010).
- [4] M. V. Koudriachova, N. M. Harrison, and S. W. de Leeuw, *Phys. Rev. B* **65**, 235423 (2002).
- [5] M. V. Koudriachova, N. M. Harrison, and S. W. de Leeuw, *Solid State Ionics* **157**, 35 (2003).
- [6] F. Gligor and S. W. de Leeuw, *Solid State Ionics* **177**, 2741 (2006).
- [7] M. V. Koudriachova, N. M. Harrison, and S. W. de Leeuw, *Phys. Rev. Lett.* **86**, 1275 (2001).
- [8] A. Stashans, S. Lunell, R. Bergström, A. Hagfeldt, and S. E. Lindquist, *Phys. Rev. B* **53**, 159 (1996).
- [9] T. L. Chan and J. R. Chelikowsky, *Nano Lett.* **10**, 821 (2010).
- [10] Q. F. Zhang, W. X. Zhang, W. H. Wan, Y. Cui, and E. Wang, *Nano Lett.* **10**, 3243 (2010).
- [11] M. Anicete-Santos *et al.*, *Phys. Rev. B* **77**, 085112 (2008).
- [12] S. Sharma, J. K. Dewhurst, and C. Ambrosch-Draxl, *Phys. Rev. B* **70**, 104110 (2004).
- [13] J. S. Braithwaite, C. R. A. Catlow, J. D. Gale, and J. H. Harding, *Chem. Mater.* **11**, 1990 (1999).
- [14] A. R. Armstrong, C. Lyness, P. M. Panchmatia, M. S. Islam, and P. G. Bruce, *Nature Mater.* **10**, 223 (2011).
- [15] P. Gibot *et al.*, *Nature Mater.* **7**, 741 (2008).
- [16] C. Delmas, M. Maccario, L. Croguennec, F. Le Cras, and F. Weill, *Nature Mater.* **7**, 665 (2008).
- [17] J. Y. Huang *et al.*, *Science* **330**, 1515 (2010).
- [18] See supplemental material at <http://link.aps.org/supplemental/10.1103/PhysRevLett.106.248302> for experimental details and additional results showing the different charging behaviors under end-contact and side-contact configurations.
- [19] Y. M. Chiang, *Science* **330**, 1485 (2010).
- [20] T. Song *et al.*, *Nano Lett.* **10**, 1710 (2010).
- [21] H. Iwanaga, M. Egashira, K. Suzuki, M. Ichihara, and S. Tacheuchi, *Philos. Mag. A* **58**, 683 (1988).
- [22] K. Suzuki, M. Ichihara, and S. Takeuchi, *Philos. Mag. A* **63**, 657 (1991).
- [23] M. Legros, G. Dehm, E. Arzt, and T. J. Balk, *Science* **319**, 1646 (2008).
- [24] O. W. Johnson, *Phys. Rev.* **136**, A284 (1964).
- [25] M. A. Reddy *et al.*, *Electrochem. Comm.* **8**, 1299 (2006).
- [26] D. Larcher *et al.*, *J. Electrochem. Soc.* **150**, A133 (2003).
- [27] Y. S. Hu, L. Kienle, Y. G. Guo, and J. Maier, *Adv. Mater.* **18**, 1421 (2006).
- [28] E. Baudrin *et al.*, *Electrochem. Comm.* **9**, 337 (2007).
- [29] S. Bach, J. P. Pereira-Ramos, and P. Willman, *Electrochim. Acta* **55**, 4952 (2010).
- [30] G. Jain, M. Balasubramanian, and J. J. Xu, *Chem. Mater.* **18**, 423 (2006).
- [31] N. A. Milne, M. Skyllas-Kazacos, and V. Luca, *J. Phys. Chem. C* **113**, 12983 (2009).